*Mausam*, (1991), **42**, 2, 131-138

551.511.13 : 551.553.21 (267)

# Thermohaline structure in the equatorial Indian Ocean during Monsoon-77

R. R. RAO, K. D. K. M. SARMA and BASIL MATHEW

*Naval Physical and Oceanographic Laboratory, Cochin*

(*Received 28 March 1989*)

**सार** — मानसून-77 (1977 के मई के अन्त/जून के आरम्भ में) के फील्ड प्रेक्षण प्रोग्राम के दौरान सोवियत संघ के पोतों द्वारा, विषुवतीय हिन्द महासागर (70°पू० और 90° पू० के मध्य) में तीन जोनीय ट्रांजेक्टों (2° उ० तथा 2° द०) के साथ ऊपरी 200 मी० जल कॉलम में जल आरेखीय और बी० टी० डेटा सेट इकट्ठे किए गए। इनसे सतही पूर्वी विषुवतीय जेट के साथ सम्बद्ध तापप्रवणता के मुख्य पूर्वाभिमुख अवदाब का पता चला है। मध्य हिन्द महासागर में, मई 1977 के अन्त से दो महीनें की अवधि में ग्रीष्म मानसून के आरम्भ और समाप्ति पर शीतलन और गहरेपन की मिश्रित स्तरों की दरें क्षीण थीं। किन्तु ऊपरी 200 मी० जल कॉलम के खारेपन में अपेक्षाकृत महत्वपूर्ण परिवर्तन देखे गए। इस क्षेत्र में जुलाई 1977 के अन्तिम सप्ताह के दौरान, नेट सतह ऊष्मा के अनुसार, सिनॉप्टिक माप पर समुद्र सतह तापमान में हल्की सी वृद्धि हुई।

ABSTRACT. The hydrographic and BT data sets collected in the upper 200 m water column along three zonal transects (2°N, equator and 2°S) in the equatorial Indian Ocean (between 70°E and 90°E) made by USSR ships during the field observational programme of Monsoon-77 (end May/early June 1977) showed prominent eastward depression of thermocline in association with the surface easterly equatorial jet. In the central Indian Ocean, the mixed layer cooling and deepening rates were weak with the onset and sway of the summer monsoon over a two month period from end May 1977, but relatively significant changes were noticed in the salinity of the upper 200 m water column. In this region, cn a synoptic scale a mild increase in SST is in accordance with the net surface heat gain during the last week of July 1977.

**Key words** — Pressure gradient, salinity, surface heat budget, thermohaline, thermocline.

## 1. Introduction

In the tropics the characteristic response times of baroclinic ocean processes are much closer to the time scales of the variability of the surface wind field (Leetma *et al.* 1981). The seasonal variability in the east-west slope of the tropical thermocline appears to be in phase with changes in zonal wind stress. When the trades are strongest the tilt of the thermocline is largest and *vice versa*. However, the mean east-west surface wind stress over the equatorial Indian Ocean for most of the year is small (Hastenrath and Lamb 1979). In the transition between the two monsoons, *i.e.*, April-May and October-November, well defined westerly winds appear along most of the equator. Associated with these is an eastward narrow oceanic jet and a simultaneous rise in the sea level and a depression in the thermocline off Sumatra (Wyrtki 1973). The jets are strongest between 2°N and 2°S. Direct current measurements for nearly two years near Gan island clearly showed the appearance of the jets in the upper layers with speeds in excess of 100 cm/s approximately in phase with the local east-west components of the wind stress (Knox 1976). Recent drift buoy measurements also confirmed an eastward flow along the equator (Cresswell *et al.* 1981, Reverdin *et al.* 1983). Polonoskiy and Shapiro (1983) observed an eastward flow in the top 100 m water column from 26 April to 19 May 1980 at 61° E at the equator. Nearly after two months, the flow reversed towards west in the upper 55 m water column during 13 July to 2 August 1980 at this location. Associated with the jet are variations in the large transport of water and in the depth of a mid-thermocline isotherm (20° C) by as much as 40 m over large areas (Wyrtki 1973). The formation of this eastward jet is accompanied by the convergence of currents along the equator, which leads to the deepening of the quasi-isothermal layer with a sharp thermocline below. The CTD casts made during December 1976-January 1977 showed such a sharp thermocline east of 73° E (Eriksen 1979). The equatorial jets are undoubtedly part of forced dynamic response to local wind stress, and they in turn appear to be responsible for the large scale re-distribution of mass (as indicated by changing thermocline depth and structure) and water types (*e.g.*, appearance of Arabian Sea water from 70° E to 90°E along the equator, Wyrtki 1973). The dynamics of this response are far from understood; indeed the phenomena are not even adequately described by measurements (Eriksen 1979).

The equator acts as a wave guide. Flow changes induced by the presence of coast lines, variability in wind patterns and instabilities of the current system tend to propagate along the equator ( Moore and Philander 1977). Several observations revealed that equatorial waves occur in a very broad spectrum, from 2-3 days to an year (Wunsch 1978, Weisberg *et al.* 1979, Eriksen 1981, Luyten and Roemmich 1982). During the summer monsoon, the observed variability in the upper layers of the central and eastern equatorial

Indian Ocean could be larger due to well known propagating wave disturbances along the equatorial wave guide (Lighthill 1969). Enough data were not collected to substantiate this type of short term variability. In the present study, the observed variability in the thermohaline fields along the equatorial band during end May to early June 1977 (pre-onset regime), the observed temporal changes in the vertical thermohaline profiles from end May to end July 1977 (pre to post onset regime) and the observed short term variability 0 (1 week) in the central equatorial Indian Ocean at a stationary polygon during end July 1977 are documented with the aid of data sets collected during Monsoon-77 field experiment.

## 2. Observations

Under the aegis of Monsoon-77, four USSR ships made three westward transects along 2°N, equator and 2°S from 90°E to 70°E during 27 May to 2 June 1977 occupying hydrographic stations approximately 60 to 120 nautical miles apart along each transect. These ships formed a stationary polygon over the central equatorial Indian Ocean (Fig. 1) from 24 to 31 July 1977. Time series measurements of all standard surface marine meteorological elements inclusive of solar radiation at one hourly intervals, BT and hydrocasts at three hourly intervals were made at all the locations. In the following discussion, the corners of the polygon counting clockwise from northern location are designated as N, E, S and W locations. Temperature measurements across the equator along 84°E made during last week of May 1964 during IIOE were also made use of.

## 3. Results and discussion

### 3.1. *Thermal structure along the equatorial belt*

Temperature sections (Fig. 2) constructed along the equator (1°N to 1°S) utilising the temperature climatology of Levitus (1982) clearly show the eastward deepening of the thermocline. A dramatic increase in the zonal slope from April to May is very prominent. This steep slope persisted during June and relaxed only during July.

The hydrocast data collected during Monsoon-77 along three zonal transects (2°N, 0° and 2°S) are utilised to construct depth-longitude fields of temperature [Fig. 3(a)] and salinity [Fig. (3b)] in the upper 200 m water column. In all three sections, the eastward depression of thermocline is prominently noticed. These slopes are relatively steeper to those reported by Taft and Knauss (1967) along the equator during 24 Feburary to 10 April 1963. These slopes would probably strengthen under the forcing of the strong equatorial westerly winds which produce the equatorial easterly jet. However, the zonal thermal sections along the equator are typical when compared to that along either 2°N or 2°S. The surface mixed layer is deeper and the thermocline (in particular the water column sandwiched between 26° and 16° C isotherms) is very sharp along the equator compared to that either along 2°N or 2°S. Thus the upper boundary of this sharp thermocline is depressed along the equator, with no perceptible differences in the lower boundary of the sharp thermocline say the 16°C isotherm) all along the three transects.

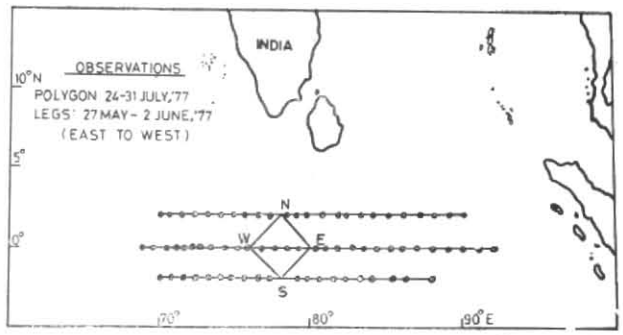


Fig. 1. Station location map

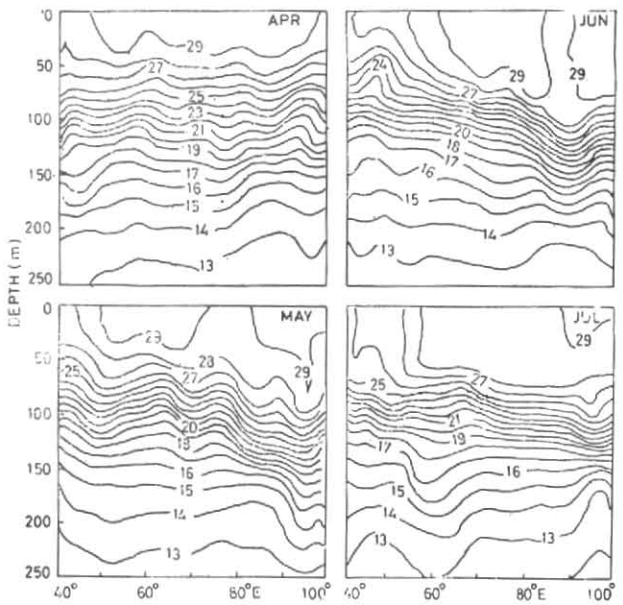


Fig. 2. Mean monthly depth longitude temperature (°C) along the equator

Based on another independent data set collected onboard *Pioneer* (supplied by NODC), the transequatorial temperature section along 84°E during 24-31 May 1964 (Fig. 4) also confirms these features. Similar features were observed along 88° E during the same period (Muraleedharan *et al.* 1980). The orientation of isotherms along this section suggests that the easterly equatorial jet could be very narrow and strong in the near vicinity of the equator (between 2°N and 2°S) and is maintained by convergence along the equator. The multi year average of surface current field of Cutler and Swallow (1984) corresponding to the last 10-day period of May and the first 10-day period of June and drifting buoy trajectories (Reverdin *et al.* 1983) also confirm this feature.

### 3.2. *Salinity structure along the equatorial belt*

During July 1962, the upper 100 m water column east of 73°E showed salinities $< 35‰$ (Taft and Knauss 1967). Between 100 and 150 m depths a thin core of high salinity $> 35.2‰$ embedded between two isohalines of $35.1‰$ suggest the presence of eastward advection of Arabian Sea water. Further the tongue shaped eastward protrusion of $35.2‰$ waters below 100 m depth east of 73°E also support sub-surface eastward

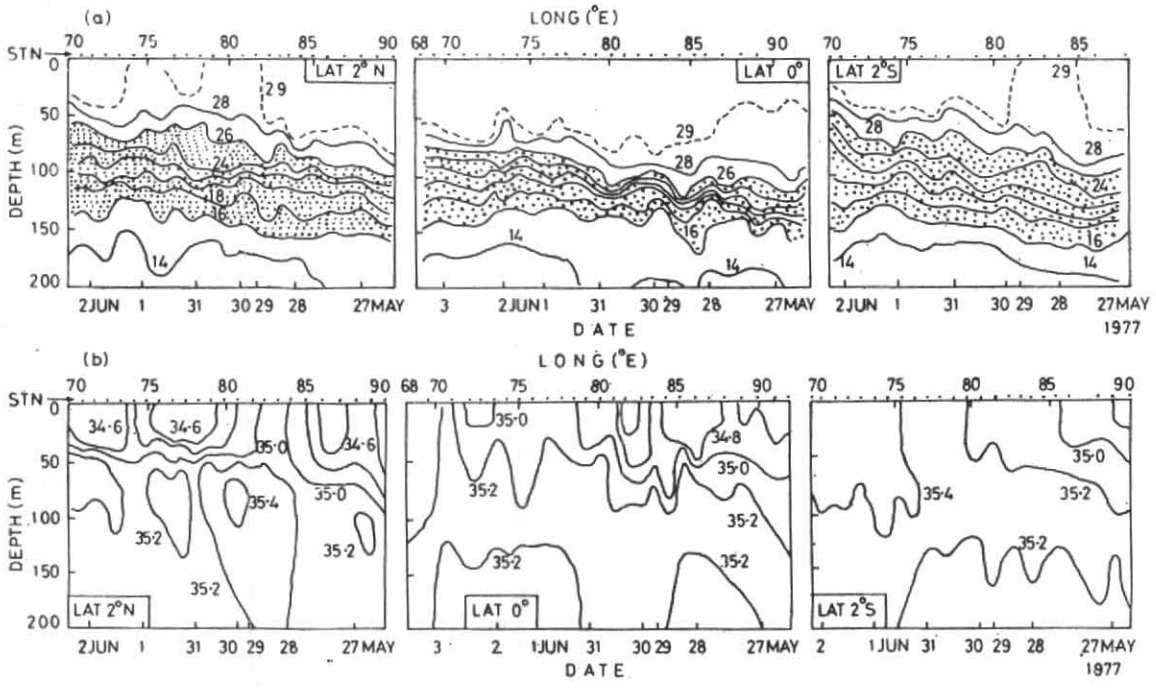


Figs. 3 (a&b). East-west upper ocean : (a) thermal & (b) salinity structure in the central equatorial Indian Ocean

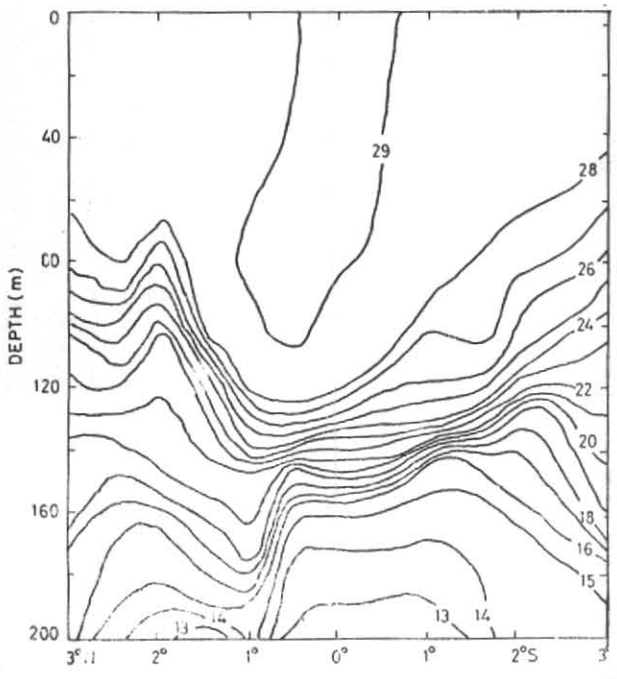


Fig. 4. Transequatorial thermal structure along 84°E during 24-31 May 1964

flow between 100 and 150 m depths. The easterly jet noticed by Wyrtki (1973) is a plausible mechanism for transporting the high saline water from the western part of the ocean through the Maldives to nearly 90°E.

In the present study the salinity regime in the upper 200 m water column shows an increase with depth along all the three transects. The low saline ($<35‰$) surface waters are probably of southern hemispheric origin (Fieux and Levy 1983) while the high saline ($>35‰$) waters are of Arabian Sea origin. The *T-S* analysis (Fig. 5) shows that sub-surface salinity maxima occurring about $\sigma_t = 23.6$ g/l level ($\sim$ 400 cl/t) obviously belongs to the Arabian Sea High Salinity Watermass (ASHSW) (Wyrtki 1971). The differences in the distribution of ASHSW at different locations could be attributed to the unequal spreading of ASHSW especially east of Maldive Islands. The *T-S* diagrams suggest that above $\sigma_t$=25 g/l, the waters are more homogeneous in salinity at the equator compared to either 2°N or 2°S. The thickness of low saline waters $<35‰$ in the surface layer decreased southward. The meridional gradient in the salinity regime of the surface layers is larger in the western sector compared to that of the eastern sector. These longitudinal differences might have been resulted due to the eastward flowing Arabian Sea high saline waters.

### 3.3. *Equatorial transport estimates*

Geostrophic currents relative to 200 db between 0° and 2° N/2° S are estimated for different pairs of stations within a 5° zonal grid and the averaged net transports are presented in Table 1. The standard geostrophic methodology was followed in the present estimates. Joyce *et al.* (1986) have shown only a 10% deviation between directly measured and geostrophic transport estimates even near the equator. Between 70° and 85° E, the average surface velocity is around 110 cm/s which is comparable to the earlier estimates of equatorial jet (Wyrtki 1973, Knox 1976). However, such strong currents are absent east of 85° E where a relatively weaker eastward flow is noticed. This is in good agreement with the ship drift climatology of this region (Cutler and Swallow 1984). The reasons for the eastward increase north of the equator and eastward decrease south of the equator in the velocity/transport of the flow are, however, not clear. The estimated

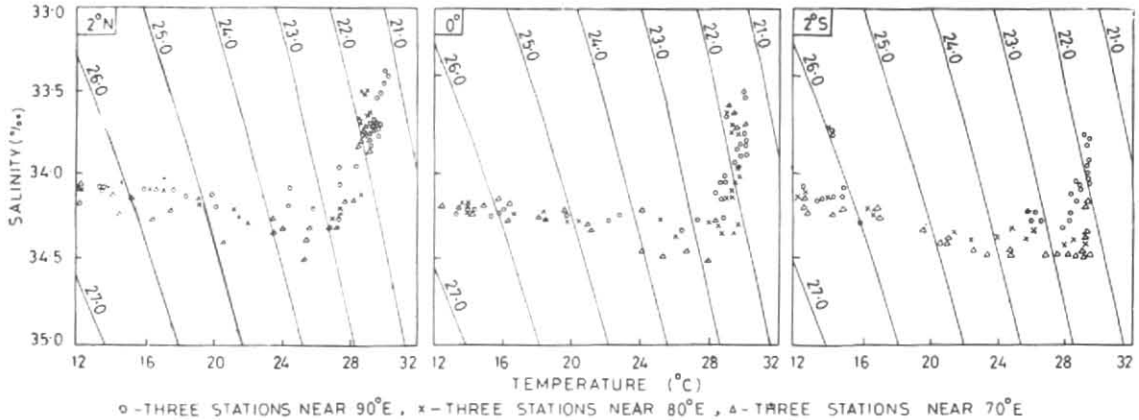


Fig. 5. *T-S* diagrams for typical locations along : (a) 2° N, (b) 0°, and (c) 2° S

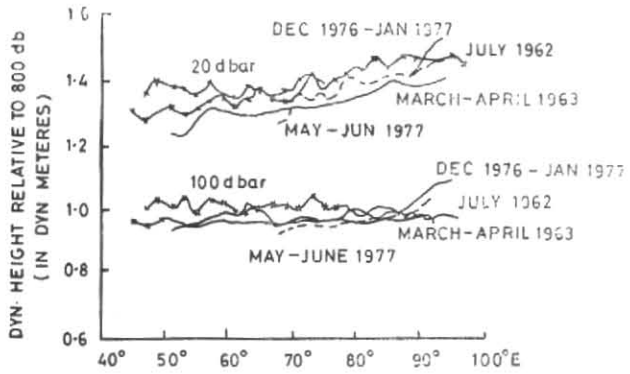


Fig. 6. Dynamic height (dyn. m) at the surface relative to 800 db

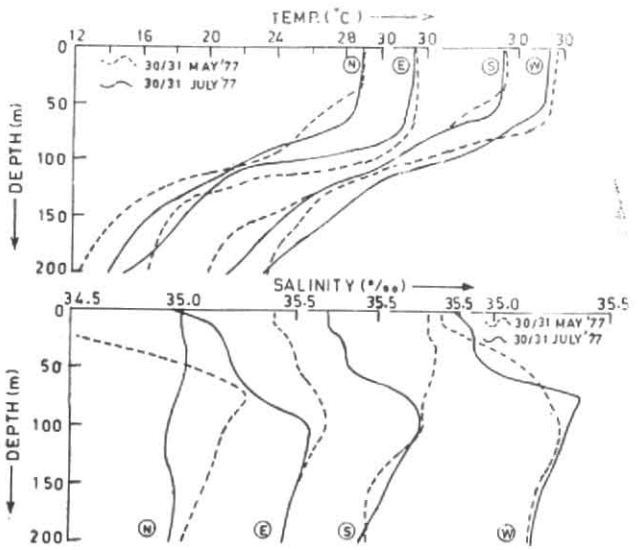


Fig. 7. Typical pre-onset and post-onset vertical profiles of temperature and salinity at the stationary polygon

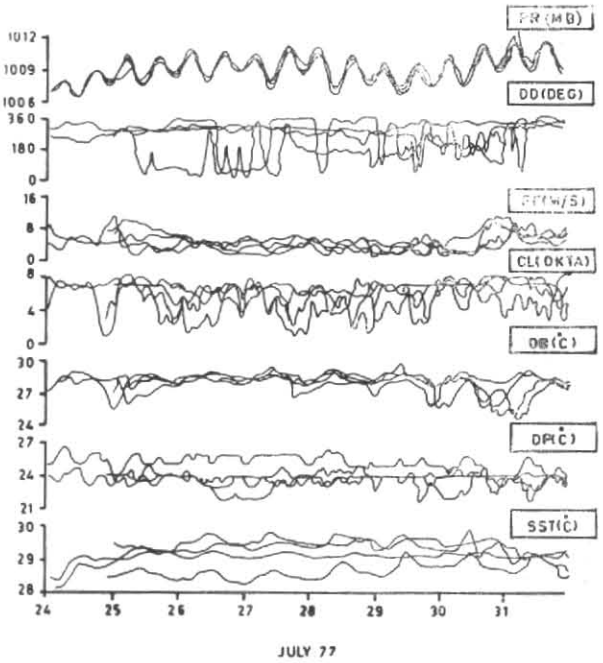


Fig. 8. Hourly march of surface marine meteorological elements at the stationary polygon

TABLE 1

**Geostrophic currents (cm/s) relative to 200 db and the net transport between 2° N & 0° and 0° & 2° S ($10^6 m^3/s$) averaged over 5° zonal bands (in brackets)**

| | 70°-75°E | 75°-80°E | 80°-85°E | 85°-90°E |
|---|---|---|---|---|
| 0°-2°N | 36 | 98 | 172 | 0.6 |
| | (8.20) | (22.3) | (38.4) | (1.32) |
| 0°-2°S | 156 | 137 | 73 | 33 |
| | (33.7) | (29.3) | (16.2) | (7.9) |

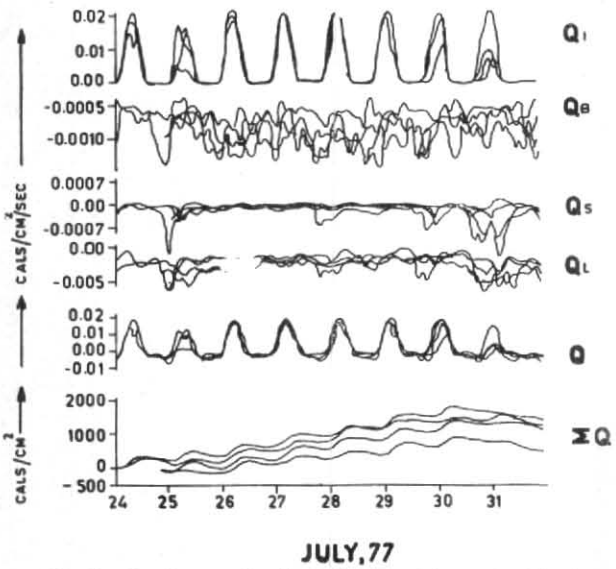


Fig. 9. Hourly march of surface heat budget estimates at the stationary polygon

eastward transport is about twice the estimate ($22.5\times 10^6$ m³/s) of Wyrtki (1973). The present study indicates that the jet is about 150 m deep while Wyrtki (1973) assumed that it is of the order of 60 m.

### 3.4. *Zonal pressure gradient along the equator*

The near surface zonal pressure gradient along the equator in the Indian Ocean is not only westward but also the steepest observed which is apparently related to the inter-monsoonal westerly winds along the equator (Eriksen 1979). Both in the Atlantic and Pacific Oceans the surface pressure gradient along the equator is eastward. Eriksen (1979) presented the dynamic height at 20 db and 100 db relative to 800 db for all the then available three transects along the equator in the Indian Ocean. The dynamic height distribution at 20 db and 200 db relative to 800 db are presented along with Eriksen's (1979) diagram for easier comparison purposes (Fig. 6). During May-June at 20 db the dynamic height increases by about 20 dyn cm from 68° E to 90° E which is lower than the value of 25 dyn cm for December-January (Eriksen 1979). Over the same region the transects of Taft and Knauss (1967) showed a dynamic height increase of 12 dyn cm during July 1962 and 8 dyn cm in March-April 1963.

The present data set showed a pressure gradient of $-8\times 10^{-5}$ dyn/g for the region between 68° E and 90° E which is less than $-10\times 10^{-5}$ dyn/g, in December-January (Eriksen 1979) relative to 800 db. Weisberg and Weingartner (1986) summarised the results of pressure gradient computations along the equator in all the three oceans. Their study has shown that both in the Atlantic and Pacific the large scale pressure gradient along the equator varied between $1\times 10^{-5}$ to $7\times 10^{-5}$ dyn/g during major part of the year with few exceptions. The pressure gradient along the equator in the Indian Ocean both during December/January and May-June are much stronger (although opposite in sign) than those in the Atlantic and Pacific. The slightly weaker pressure gradient during May/June compared to that during December/January probably

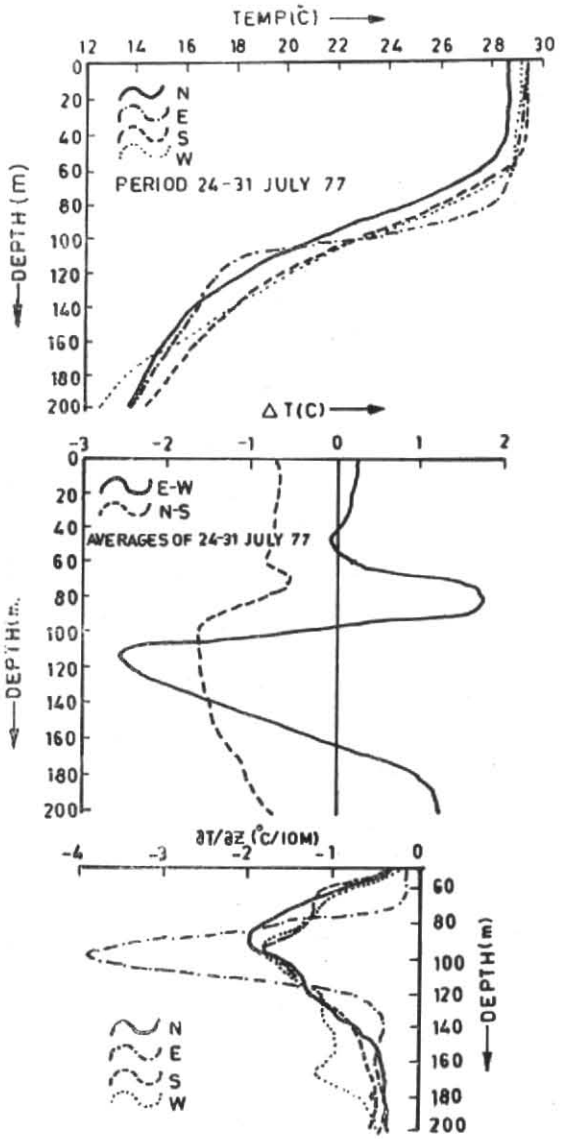


Fig. 10. Mean vertical BT profiles, lateral temperature differences, vertical thermal gradients during 24-31 July 1977 over the polygon

suggest that the equatorial jet is stronger during autumn transition compared to that during spring transition as inferred by Eriksen (1979).

### 3.5. *Variability in the vertical temperature and salinity profiles with the onset and sway of the summer monsoon*

The onset and sway of the summer monsoon is known to produce dramatic variations in the thermal structure of the upper layers in the northern Indian Ocean (Wyrtki 1971). The surface mixed layer cooling and deepening are prominent of the north Indian Oceanic response to the summer monsoonal forcing. However, the monsoonal forcing is relatively weaker over the central equatorial Indian Ocean (Hastenrath and Lamb 1979) leading to weaker oceanic response. Inspite of this weaker forcing over this region, McPhaden (1982) found that 80% of the variance observed in the seasonal cycle of SST could be explained in terms of one dimensional processes. The horizontal advection

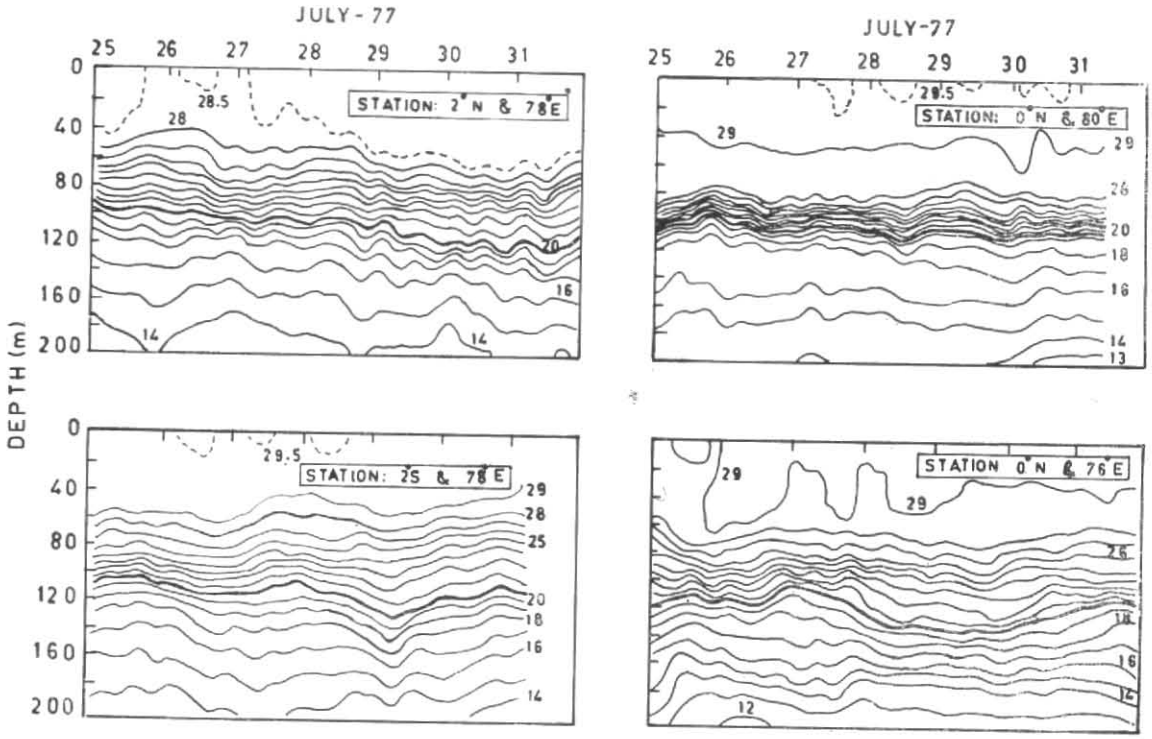


Fig. 11. Depth-time temperature fields at N, E, S and W respectively during 24-31 July 1977

assumes less importance even under the presence of swift east-west currents on account of weak zonal thermal gradients.

The typical vertical thermal profiles corresponding to 30/31 May 1977 (average of three profiles nearest to the station) and 30/31 July 1977 (average of 16 time series profiles) of temperature and salinity are shown in Fig. 7. The mixed layer cooling was minimal at all four locations while the layer deepening was relatively larger at the stations away from the equator. These features clearly reflect the weak local response of the surface layer in the central equatorial Indian Ocean to the summer monsoonal forcing. The salinity distribution in the upper layers of the ocean is known to be influenced by evaporation, rainfall, river run-off and advection of low/high saline waters etc. Unfortunately no quantitative figures are available on the magnitudes of these processes to assess their relative importance. Under these circumstances one can at best qualitatively link up the salinity variations with some of the known seasonal processes. In addition, in areas where inter-annual variability is large, this type of approach further leads to uncertainity. Knox (1976), for example, reported large differences between the observed equatorial undercurrent near Gan island (00°41'S, 73° 10'E) in the equatorial Indian Ocean during 1973 and 1974. These constraints have to be borne in mind while interpreting the temporal variations in the observed salinity profiles. The temporal variations over a period of two months were distinctively larger in the topmost 100 m water column at E and S. This variability was largest at the surface and decreased with depth at these two locations. At W the change was not significant while at N there was significant changes throughout the 200 m water column. The mean salinity in the upper 100 m water column decreased at E and S from end May to end July 1977. To gain a description on the prevailing circulation along the equator the following from Cutler and Swallow (1984) is reproduced here. "Eastward flow (equatorial jet) can just be detected in early April between 70° and 90° E. It is definitely present in mid April and by late April extends from 55° to 95° E. This continues steadily until early June when decay sets in from the eastern end. By late June it has practically disappeared. Weak westward flow is again seen between 60° E and 75° E during July and August". Due to the disappearance of this equatorial jet from late June and weak westward flow (Polonskiy and Shapiro 1983) during July could advect low saline waters into the study area. The local summer monsoonal rainfall would also contribute to the dilution of surface waters. These above arguments support the observed changes only at E and S. At N, a sharp halocline is noticed between 20 and 75 m depths during end May 1977. Such a halocline with moderate intensity is seen in the profiles only at E and W. Although there is some similarity between the salinity profile at N with those of the other locations during end May 1977, such resemblence is totally absent in the corresponding profiles of end July 1977. The reasons for the formation of a near isohaline water column at N are not clear though lateral advection could be a strong possibility.

### 3.6. *Short-term (synoptic scale) variability*

#### 3.6.1. *Surface heat budget*

As the coupling between the local wind stress and the upper oceanic response is quite strong in the tropics, it would be worthwhile to gain a description on the surface meteorological conditions prevailed during

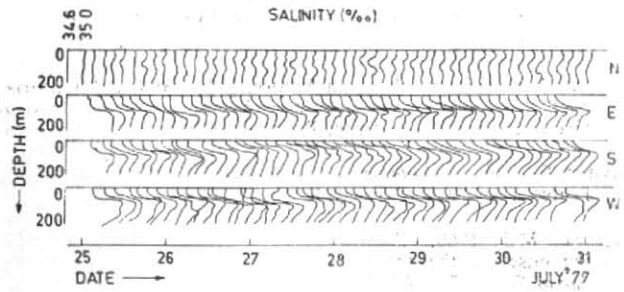


Fig. 12. Three hourly vertical salinity profiles over the polygon during 24-31 July 1977

the observational period in order to link up the subsurface variability. The surface pressure exhibited a rhythmic fluctuations with a range of 6 mb (Fig. 8). The wind direction (DD) was rather unsteady while the wind speeds (FF) exhibited a good coherence over the array. The dew point temperature (DP) was relatively steady although weak spatial differences persisted. The sea surface temperature (SST), in general, showed a mild warming tendency throughout with the only exception on 31 July. The lateral gradients in SST were also relatively small within the observational array.

All the terms of the heat budget equations with the only exception of insolation are derived with the aid of empirical relationships (Fig. 9). The observed solar radiation ($Q_I$) data were corrected for the surface reflective losses with the observed albedo data while the heat loss terms as net long wave radiation ($Q_B$), sensible heat flux ($Q_S$) and latent heat flux ($Q_E$) were estimated following Rao *et al.* (1985). The $Q_I$ shows a standard pattern with some differences within the array when the wind speed was relatively larger (24, 25, 30, 31 July 1977). The $Q_B$ distribution appears to be chaotic as a reflection of cloudiness for which it is corrected. The $Q_S$ was mostly negative implying an unstable regime. The pattern of $Q_E$ dominated other loss terms in the distribution of $Q$. The accumulative heat gain ($\Sigma Q$) from 24/25 July showed a progressive increase with time. The differences within the array towards the end of the observational period are caused due to both variable surface heat flux terms as well as differences in the starting times. An accumulation of 1000 cal/cm² over a 8-day period imply an average daily gain of about 125 cal/cm²/day over this array. Thus the observational area experienced relatively undisturbed weather with a net accumulation of heat which is also reflected in the increase of SST (Fig. 5) suggesting the importance of local one dimensional processes on short time scales.

### 3.6.2. *Upper ocean thermal structure*

The temporal averaged (24-31 July) vertical thermal profiles constructed with BT data reveal the typical structure of the temperature distribution in the topmost 200 m water column in the observational array (Fig. 10). The near surface mixed layer thickness was around 60 m with the temperature differences of about less than 1°C within the polygon. The mixed layer at E was deeper by about 10 m. The thermocline slopes were similar with the only exception at E where unusually steep gradient as large as 4°C/10 m around 100 m depth was noticed (Fig. 9). The corresponding vertical thermal gradient ($\partial T/\partial z$) at the other three locations was of the order of 2°C/10 m at this depth. The presence of such sharp gradient at E and its absence at W which is closer to the Maldive islands is quite intriguing. The meridional thermal gradient in the upper 200 m water column was of the order of 1°C/440 km with higher temperature towards south while the zonal thermal gradient varied with depth. The zonal thermal gradient appears to have been influenced by the unusually strong $\partial T/\partial z$ at E, which was similar to that of in July 1962 (Wyrtki 1971). The peaks in $\partial T/\partial x$ occurred at 80 m and 120 m depths with almost vanishing gradients at 100 m. This implies that the isotherms sloped down eastward above 100 m and *vice versa* below this depth with maximum slopes occurring at 80 and 120 m depths suggesting a change in the direction of currents below 100 m.

### 3.6.3. *Variability in the upper ocean temperature and salinity regimes*

The short-term variability in the thermal regime in the upper 200 m water column at the four corners of the polygon during the observational period is shown in Fig. 11. The isotherms were contoured at 1° C interval in the depth-time domain. These sections clearly reveal the nature of spatial heterogeneity within the polygon area. In addition to the differences noticed in the mixed layer, considerable differences are also evident in the thermocline. At E the sharp vertical thermal gradient showed a progressive diffusion with time. The core isotherms of 19°C and 26°C, however, did not exhibit any significant changes in depth with time. But the vertical separation between 28°C and 17°C isotherms nearly doubled during this period. At N the thermocline progressively deepened with time. These changes are probably associated with the dynamics of the eastward flowing monsoon current during this period. However, the present data set is hardly adequate to address this problem in any detail. Short period fluctuations probably forced by semi-diurnal tides are present in all the sections.

The three hourly march of vertical salinity profiles derived from hydrocasts at all the four locations are portrayed in Fig. 12. The dissimilar nature of the salinity profiles at N is quite conspicuous. The profiles at this location do not exhibit any halocline while all the other locations show halocline with variable gradient. The subsurface salinity maxima at E, S and W is associated with the Arabian Sea High Salinity watermas (ASHSW) occurring around 400 cl/t surface (Wyrtki 1971, Rao *et al.* 1990).

## 4. Conclusions

In the equatorial Indian Ocean eastward depression of thermocline is prominent during May/June. Very sharp thermocline with deep mixed layer was noticed only along the equator compared to 2° N and 2° S transects suggesting that the equatorial jet is confined to the near vicinity of the equator. Surface velocity from geostrophic computations between 70°E and 85° E showed an average of 110 cm/s which is in broad agreement with previous observations. However, currents were weaker east of 85° E probably because the decay

of equatorial jet might have started in the eastern Indian Ocean by end May/early June. The zonal pressure gradient along the equator between 70 and 90° E was $-0.8\times10^{-5}$ dyn/g which was slightly lower than the value of $-10\times10^{-5}$ dyn/g reported along equator in the Indian Ocean for December 1976-January 1977. This probably suggests that the equatorial jet is stronger during the autumn transition that in the spring transition.

In the polygon area surface mixed layer cooling was minimal and the layer deepening was marginal from end May to end July 1977, suggesting a weak thermal response of the central equatorial Indian Ocean to the summer monsoonal forcing. But relatively larger changes are noticed in the vertical salinity profiles especially in the top 100 m during this two month period.

The time series of marine meteorological elements collected during the last week of July 1977 showed fair weather conditions although weak unstable regime continued throughout. One dimensional heat exchange processes produced an accumulation of heat of the order of 125 cal/cm²/day causing an increase in SST suggesting the importance of local air-sea interaction processes on a synoptic scale.

*Acknowledgements*

We are thankful to all scientists and technicians who have contributed for the collection and processing of the data sets utilised and to the Project Director of Monex for its supply. We thank to the Director, Naval Physical and Oceanographic Laboratory for all the facilities and encouragement. We are grateful to the anonymous reviewer for valuable comments.

**References**

Cresswell, G.R., Fieux, M. and Gonella, J., 1981, "The Wyrtki Equatorial Jet May/June 1980", *Tropical Atmosphere News Letter*, **5**, 3 (unpublished manuscript).

Cutler, A. N. and Swallow, J.C., 1984, *Surface currents of the Indian Ocean (to 25 S, 100 E) : Compiled from historical data archived by Meteorological Office*, Bracknell, U. K. Institute of Oceanographic Sciences Rep. No. 187, 8 pp and 36 charts.

Eriksen, C., 1979, "An equatorial transect of the Indian Ocean", *J. Mar. Res.*, **37**, 215-232.

Eriksen C., 1981, "Deep currents and their interpretation as equatorial waves in the western Pacific Ocean", *J. Phys. Oceanogr.*, **11**, 48-70.

Fieux, M. and Levy, C., 1983, "Seasonal observations in the western Indian Ocean", In *Hydrodynamics of the Equatorial Ocean*, Ed. Nihoul, J.C.J., Elsvier Oceanography Series No. 36, 17-29.

Hastenrath, S. and Lamb, P.J., 1979, "*Climatic Atlas of the Indian Ocean*, Part I, Wisconsin Univ. Press, USA.

Joyce, T.M., Lukas, R. and Firing, E., 1986, "On the hydrostatic balance and equatorial geostrophy", *Deep-Sea Res.*, **35**, 1255-1258,

Knox, R.A., 1976, "On a long series of measurements of Indian Ocean equatorial currents near Addu Atoll", *Deep-Sea Res.*, **23**, 211-221.

Leetma, A., McCreary, J.P. and Moore, D.W., 1981, "Equatorial currents : Observations and Theory", In *Evolution of Physical Oceanography*, Ed. Warren, B.A. and Wunsch, C., 184-196.

Levitus, S., 1982, *Climatological Atlas of the World Ocean*, NOAA Professional Paper, No. 13, Rockville Md, 173 pp.

Lighthill, M.J., 1969, "Dynamic response of the Indian Ocean to the onset of the southwest monsoon", *Philosophical Trans. Royal Soc.*, **A265**, 45-92.

Luyten, J.R. and Roemmich, D.H., 1982, "Equatorial currents at semi-annual periods in the Indian Ocean", *J. Phys. Oceanogr.*, **12**, 406-413.

McPhaden, M.J., 1982, "Variability in the central equatorial Indian Ocean, Part II : Oceanic heat and turbulent energy balances", *J. Mar. Res.*, **40**, 406-413.

Moore, D. and Philander, S.G.H., 1977, "Modelling of the tropical oceanic circulation", In *The Sea*, **6**, Wiley Interscience, New York, 319-361.

Muraleedharan, P.M., Nair, R.N. and Basil Mathew, 1980, "Some studies on the Equatorial Undercurrent and Equatorial Jet in the Indian Ocean", *Bull. Dep. Mar. Sci.*, **13**, 113-126.

Polonskiy, A.B. and Shapiro, M.B., 1983, "Variability of hydrophysical fields in the western equatorial zone of the Indian Ocean", *Oceanology*, **23**, 172-175.

Rao, R.R., Ramam, K.V.S., Rao, D.S. and Joseph, M.X., 1985, "Surface heat budget estimates at selected areas of North Indian Ocean during Monsoon-77", *Mausam*, **36**, 1, 21-32.

Rao, R.R., Hareesh Kumar, P.V. and Basil, Mathew, 1990, "Water-mass modification in upper layers of the Arabian Sea during ISMEX-73", *Mausam*, **41**, 4, 611-620.

Reverdin, G., Fieux, M., Gonella, J. and Luyten, J.R., 1983, "Free drifting buoy measurements in the Indian Ocean Equatorial Jet", In *Hydrodynamics of the Equatorial Ocean*, Ed. Nihoul, J.C.J. Elsvier Oceanography Series, **36**, 99-120.

Taft, B.A. and Knauss, J.A., 1967, "The Equatorial Undercurrent of the Indian Ocean as observed by the Lusiad Expedition", *Bull. Scripps Inst. Oceanogr.*, **9**, 167 pp.

Weisberg, R.H., Horigan, A. and Colin, C., 1979, "Equatorially trapped Rossby-gravity wave propagation in the Gulf of Guinea, *J. Mar. Res.*, **37**, 67-86.

Weisberg, R.H. and Weingartner, T.J., 1986, On the baroclinic response of the zonal pressure gradient in the equatorial Atlantic Ocean, *J. Geophys. Res.*, **91**, 11717-11725.

Wunsch, C. 1978, "Observations of equatorially trapped waves in the ocean : A review prepared for equatorial workshop, July 1977", In, *Review papers of Equatorial Oceanography*, NOAA/NYIT Univ. Press, Fort Lauderdale, 37 pp.

Wyrtki, K., 1971, *Oceanographic Atlas of the International Indian Ocean Expedition*, National Science Foundation, Washington, D.C., 531 pp.

Wyrtki, K., 1973, "An Equatorial Jet in the Indian Ocean", *Science*, **181**, 262-264.